:eedings of the First Pacific/Asia Offshore Mechanics Symposium
l, Korea, 24-28 June, 1990

OPEN CHANNEL EFFECTS IN A MATHEMATICAL MODEL AND MODIFICATION OF HARBOR

J. W. Lee
Korea Maritime University
Pusan, KOREA

STRACT

Once a mathematical model is developed
r any type of problem, it is hard to cope
th a certain modification of the original
undaries in the model. This also happens
equently in harbor design and other ocean
lated works which have very complex
ometries. This paper discusses an
proach to expansion of the boundaries in a
nerical model without changing the created
nite element mesh which fits for the given
ea.

The introduced model is an hybrid element
del and the accuracy and applicability of
e model are demonstrated for harbor
sign. The model is dealing with
nochromatic waves under linear wave
eory. In this study the boundary value
oblem of water waves scattering under the
fects of bottom friction and boundary
sorption is introduced to the model.

y Words: finite element, bottom friction,
sorption, radiation, hybrid, banded
trix, and velocity potential

NCLATURE

	Finite element region
	Incident wave amplitude
	Group velocity
	Wave celerity (phase velocity)
)	Functional
g	Gravitational acceleration
h	Water depth at (x,y)
i	$\sqrt{-1}$
K_r	Reflection coefficient
k	Wave number
x, y	Coordinate distance in horizontal direction
z	Coordinate distance in vertical direction
β	Friction coefficient
Γ	Absorption factor
γ	Phase difference of bottom friction from flow velocity
λ	Friction factor
π	The constant 3.141592654
ϕ	Two dimensional complex velocity potential function
ϕ_A, ϕ_C	Two dimensional complex velocity potential functions in the water region A and C
ω	Wave angular frequency
∇	Horizontal gradient operator
$\frac{\partial()}{\partial()}$	Partial derivative
∂A	Limit of the finite element region
∂B	Shore boundary
∂C	Limit of the super element region

INTRODUCTION

Prediction of the responses of the bay or harbor to possible incident waves both with

and without the intended design is essential for the evaluation of an existing harbor or a new harbor and its future development. Therefore, in order to more efficiently answer such questions, it is valuable to develop the best possible methods of engineering analysis. Accurate and efficient wave transformation models, either analytical, physical or numerical, are the tools needed for coastal engineering analyses.

The objective of this study is to show a numerical model for prediction of waves propagating into a bay and/or harbor with water of varying depth. Moreover, the effects of the open channel are discussed without changing the introduced grid pattern. The foundation of any wave transformation model is the wave theory upon which it is based. One of the formulations for the prediction of wave evolution is the mild-slope formulation, applicable to general linear wave theory, first developed by Berkhoff (1972). Later, this was generalized by numerous authors. This formulation already includes shoaling, diffraction, refraction and reflection phenomena. In this study, the mild-slope formulation is used for numerical analysis.

Combination of friction and absorption was done by Chen (1985, 1986) who showed several results. However, his model was restricted to using the same absorbing boundaries for the entire harbor and only for a small scale model. Furthermore, the author's study (1989) showed that the friction coefficients he used are not applicable to a fairly large area.

In this study the boundary value problem of water wave scattering under the effects of bottom friction and boundary absorption is formulated using the hybrid element method and shore boundaries are specified reasonably well together with some openings.

MATHEMATICAL FORMULATION

Generally, in the ocean, several phenomena such as superposition of waves, wave breaking, irregularity, viscosity and energy dissipation play a part in wave propagation in oceans. A numerical model taking into account all these phenomena will be very complicated. As many of these phenomena as possible will be included but the model still needs special treatment which restricts us to the modified Helmholz equation or the so-called mild-slope equation (Equation 1) for the boundary conditions such as Equations 2 through 5. This equation includes bottom friction (λ).

$$\nabla\cdot(\lambda CC_g\nabla\phi)+\frac{C_g}{C}\omega^2\phi=0 \qquad (1)$$

where ∇ denotes the horizontal gradient operator, C_g is the group velocity, C is the wave celerity, ω is the angular wave frequency, and ϕ is a two dimensional complex potential function, respectively.

The bottom friction factor λ comes from that the bottom shear stresses τ_{bj} are simplified to be linearly proportional to the horizontal velocity at the bottom ($U_j|_{z=-h}$), which includes a dimensionless spatial bottom friction coefficient β, the incident wave amplitude a_0, and the phase difference of bottom friction γ. The subscript j=1,2 denotes x and y coordinates and h is the water depth at (x,y).

$$\lambda=\frac{1}{1-i\frac{\beta a_0 e^{i\gamma}}{k\sinh kh}} \qquad (2)$$

where k is the wave number. When β=0, λ=1, then Equation 1 becomes the general mild-slope equation without the bottom friction.

Imperfect reflection at a lateral boundary is characterized by a reflection coefficient K_r, defined as the ratio of the reflected wave to the incident wave which is less than unity such as

$$\frac{\partial\phi}{\partial n}=\Gamma\phi \qquad (3)$$

where Γ is the wave absorption factor, $\Gamma=ik\frac{1-K_r}{1+K_r}$.

For perfect reflection $K_r=1$, $\Gamma=0$ and $\frac{\partial\phi}{\partial n}=0$. However, for the open channel and gaps between the breakwaters, we can have the effect of wave absorbers in the physical model by assigning $K_r=0$.

Scattered waves ϕ' in the super element region (C) satisfy the Sommerfeld radiation condition that the scattered waves must behave as outgoing waves at infinity and tend to zero as the distance tends to infinity. This condition implies that reflected waves should not return from infinity.

$$\lim_{r\to\infty}\sqrt{r}\left(\frac{\partial}{\partial r}-ik\right)\phi'=0 \qquad (4)$$

where r is the radial distance.

In order to connect the finite element area (A, the actual study area) with the outer infinite area (C) we need the continuity at the boundary between these areas such that

$$\left(CC_g\frac{\partial\phi_A}{\partial n_A}\right)=\left(CC_g\frac{\partial\phi_C}{\partial n_A}\right) \qquad (5)$$

In the theory of the calculus of variations, we can solve an equivalent problem which requires a function ϕ such that the associated functional $F(\phi)$ is stationary, instead of solving the above boundary value problem directly. The final form of the functional $F(\phi)$ is

$$F(\phi) = \int\int_A \frac{1}{2}\left\{\lambda CC_g(\nabla\phi)^2 - \frac{C_g}{C}\omega^2\phi^2\right\} + \int_{\partial A}\frac{1}{2}\lambda CC_g(\phi_c-\phi^I)\frac{\partial(\phi_c-\phi^I)}{\partial n_A} - \int_{\partial B}\frac{1}{2}\lambda CC_g\Gamma\phi^2 - \int_{\partial A}\lambda CC_g\phi_A\frac{\partial(\phi_c-\phi^I)}{\partial n_A} - \int_{\partial A}\lambda CC_g\phi_A\frac{\partial\phi^I}{\partial n_A} + \int_{\partial A}\lambda CC_g\phi^I\frac{\partial(\phi_c-\phi^I)}{\partial n_A} + \int_{\partial A}\lambda CC_g\phi^I\frac{\partial\phi^I}{\partial n_A} \quad (6)$$

where the super script I is for the incidence wave, ∂A and ∂B are the open boundary and shore boundary, respectively.

Since the functional $F(\phi)$ is stationary such that

$$\frac{\partial F}{\partial \phi_i} = 0. \quad i = 1.2.....E \quad (7)$$

$$\frac{\partial F}{\partial \mu_j} = 0. \quad j = 1.2.....m \quad (8)$$

in which E and m are the total number of nodal points and total number of unknown coefficient μ, it gives a set of linear algebraic equations for $\{\phi\}$ and $\{\mu\}$. Eliminating the constants $\{\mu\}$, the general form of an algebraic equation in matrix form can be derived as

$$[K]\{\phi\} = \{Q\}. \quad (9)$$

where K is a stiffness matrix which is a banded symmetric matrix and (Q) denotes the load vector. When solving the large system of a global stiffness matrix [K] arising from finite elements, limitations of the computer memory and CPU time require one to pay special attention to efficient programming. In this study, Equation (9) is solved for $\{\phi\}$ by dynamic block Gauss algorithm (Lee, 1989).

TESTS AND APPLICATION OF THE NUMERICAL MODEL

In order to evaluate the hybrid element solution, numerical tests are presented with regard to the sea surface fluctuations induced by a plane incident wave with two different configurations. At first, it covers the response of a fully open rectangular harbor with the consideration of an open end for the open channel effect and the wave height distribution along a detached breakwater with vertical walls.

A symmetric rectangular harbor tested has a length (l) of 31.11 cm, a width (b) of 6.04 cm, and a depth (h) of 25.72 cm. These dimensions have also been chosen by Ippen & Goda (1963) and many other researchers (Hwang et al., 1969; Lee, 1969; Hwang & Tuck, 1970, Chen & Mei, 1974; Shaw, 1976; Bettes & Zienkiewich, 1977; Ganaba et al., 1982; Chen, 1985,1986, etc). The applied area is discretized with 220 nodal points and 358 triangular elements as shown in Figure 1. Figure 2 shows response curves in case of normal incidence at the center of the inner wall. The computed results are compared with the existing theoretical and experimental results by Ippen and Goda (1963) and Lee (1969) versus kl in case that there is no friction, Γ=0. In this figure, the solid line represents the model results. The highest peak is presented at kl=1.35 and the following peaks are at kl=4.4, 8.8, etc. The present method shows good agreement with the conventional results.

In order to find the open channel effect of for this harbor the reflection coefficient K_r=0 is introduced at the inner end of the harbor. For an example case, the responses of 0.4 sec wave are shown in Figures 3 and 4. The period gives about 1.2 wavelengths inside the harbor. It can be seen that the open channel patterns (b) in Figures 3 and 4 remain approximately half of the height of the closed patterns (a).

Figure 5 shows two cases of a detached breakwater from the rectangular basin. For case I, the detached breakwater is located at the center of the mouth of the basin and each side has a gap c'=1.5L (wave length). For case II, the breakwater is located at 1.5L away from the mouth. Figure 6 shows the mesh generated for these cases. In order to compare with the result of Harms' (1980), we put the reflection coefficient K_r=0.0 along the boundary of the basin $\overline{FGHI}$ of Figure 5 to get an open channel effect in the hybrid element model. Furthermore, we assume a full reflective boundary K_r=1.0 at the straight coastline, $\overline{EF}$ and $\overline{IJ}$. Figures 7 and 8 show the results of the numerical calculations for the incoming waves normal to the detached breakwater and waves directed θ_0=45°, respectively. The present model solutions agree well the Harms' solution with surprising accuracy, except some locations due to the fact that we do not solve exactly the same problem as he does. This is due to the introduction of the full reflective straight shore boundary and narrow gaps between shore boundaries and the detached breakwater. Although there are some discrepancies in the hybrid element model, they do not indicate an error in the numerical method. They are mainly caused by the introduction of the limited basin and narrow gaps into the model.

Secondly, an asymmetric shaped harbor, Barbers Point Harbor, Oahu, Hawaii under several prototype conditions are simulated

for application but some limited results are presented.

Two sets of results are related; a) three-dimensional representation of the amplification factor for a given wave period, 15sec, and b) the harbor responses for incoming waves for various conditions. It is recalled that the test was carried out to understand some of the wave characteristics pertaining to the parameters of K_r, β, γ.

Deep Draft Harbor, which is a dredged harbor, has horizontal dimensions 610m by 550m with a depth of 11.6m. The shoreline is fairly straight, extending several miles on both sides of the harbor which fits the shore boundary condition at the super element of this numerical model (see Figure 9). The thick black line indicates the location of wave absorbers at this harbor.

The entrance channel is 1305m long, 137m wide, and 12.8m to 11.6m deep. The channel incorporates a major portion of the previous Barge Harbor. Opposite the Barge Harbor is the entrance to the West Beach Marina which is now under construction. Thus, there is a good opportunity to give the effect of this modification by putting an open segment in the model at the marina entrance without changing the grid pattern. Lee (1985) made an hydraulic model test for this area. Durham (1978) made a good analysis of harbor response for incident wave from 20 sec to 27 min for this harbor. But he did not discuss partial absorption at the shore boundary and bottom friction which give significantly different results. The finite element grid approximating the study area is presented in Figure 10.

For the numerical analysis of this problem a direction of the incoming waves near the harbor entrance from S45W is selected and waves incident with periods from 12sec to 30sec were considered in this model. Thus, the size of the element is between one-sixth (12sec) and one-sixteenth (30sec) of the incident wave length. This gives enough resolution of the wave envelopes. Wave amplitudes at each nodal point and maximum horizontal particle velocities at the centroid of each element were calculated for every 1sec increment in wave period.

Eight nodal points and element centroids were chosen for which wave amplitudes and horizontal velocities for each incident wave were presented (see Figure 10). These nodes and elements were chosen such that their locations were in harbor areas of major interest for ship berthing, navigation, and new improvement. An example of surface pattern of wave height amplification for the 15 sec incident wave, applying various values of boundary reflection, β=0.1, and $\gamma = -\frac{\pi}{4}$, are presented in Figure 11.

Plots of wave height amplification factors versus wave period for each of the selected nodal points and plots of the normalized maximum horizontal velocity versus wave period for each of the velocity stations are presented in Figures 12 and 13. Both were obtained by first using no bottom friction allowing the boundary absorption as K_r=0.98 and then letting the wave absorbers as K_r=0.9 & 0.8 under a constant bottom friction coefficient β=0.1 and a phase difference $\gamma = -\frac{\pi}{4}$. In each figure, the result with no bottom friction is represented by a solid line and those with bottom friction are represented by dotted and dashed lines varying with wave absorber and opening configurations.

CONCLUSION

The accuracy and applicability of the numerical model developed are demonstrated for harbor design or modification of harbor. It seems that the introduced open channel effect is saving the time for generation of data to be used in the mathematical model and computation.

Even though the wave absorber covered a small portion of the perimeter, we saw the effect of the wave absorbers throughout the whole area and wave frequencies selected in general. The effect of friction was significant at every station. The question of how the friction coefficient is introduced into the model can only be answered empirically either by physical model tests or by field observations.

From the application of the model, the results indicate that the combination of wave absorbers with an opening at the entrance of the West Beach Marina is more effective than the case without the opening. An interesting phenomenon found in the course of this research is that once the opening is introduced into the harbor design plan, the effect of different wave absorbers is not significant, especially at the Barge Harbor. Furthermore, at the entrance of the harbor (at station 8), there seems to be no significant difference between wave absorbers and the open case. This aspect appears not to have been previously noted by any researcher. Generally, the rate of reduction in the Deep Draft Harbor is between 20 % and 30 %. Similarly, there are minor effects at the mouth of the harbor and the Barge Harbor.

REFERENCES

Berkhoff, J. C. W. (1972), "Computation of Combined Refraction-Diffraction," Proc.

13th. Coastal Engng. Conf., Vancouver 1972, ASCE, Vol.1, pp.471-490.

Bettess, P. and Zienkiewicz, O. C. (1977), "Diffraction and Refraction of Surface Waves using Finite and Infinite Elements," Int. J. Num. Meth. Engng., Vol.11, No.8, pp. 1271-1290.

Chen, H. S. and Mei, C. C. (1974), "Oscillations and Wave Forces in a Man-made Harbor in the Open Sea," Proceeding of 10th Naval Hydrodynamics Symposium, June 1974, pp. 573-596.

Chen, H. S. (1985), "Hybrid Element Modeling of Harbor Resonance," 4th International Conference on Applied Numerical Modelling, December 1984, pp. 312-316.

Chen, H. S. (1986), "Effects of Bottom Friction and Boundary Absorption on Water Wave Scattering," Applied Ocean Research, Vol.8, No.2, pp. 99-104.

Durham, D. L. (1978), "Numerical Analysis of Harbor Oscillations for Barbers Point Deep-draft Harbor," U.S. Army Engineer Waterways Experiment Station Hydraulics Laboratory, Technical Report H-78-20.

Ganaba, M. B., Wellford, Jr. L. C., and Lee, J. J. (1982), "Dissipative Finite Element Models for Harbor Resonance Problems," Finite Element Flow Analysis (ed. Kawai, T.), University of Tokyo Press, 1982, pp. 451-459.

Harms, V. W., Safaie, B., Kam, S. N. and Westerink, J. J. (1980), "Computer Manual for Calculating Wave-height Distributions about Offshore Structures," New York Sea Grant Institute.

Hwang, L. and Tuck, E. O. (1970), "On the Oscillations of Harbors of Arbitrary Shape," J. Fluid Mech., Vol.42, Part 3, pp. 447-464.

Ippen, A. T. and Goda, Y. (1963), "Wave Induced Oscillations in Harbours: The Solution for a Rectangular Harbor connected to the Open Sea," Hydro. Lab., Massachusetts Institute of Technology.

Lee, J. J. (1969), "Wave Induced Oscillations in Harbors of Arbitrary Shape," W. M. Keck Laboratory of Hydraulic and Water Resources, California Institute of Technology, Report No. KH-R-20.

Lee, J. W. (1989), "Hybrid Element Analysis of Water Waves for Harbor Design," Ph.D. Disser., Department of Ocean Engineering, University of Hawaii.

Lee, T. T. (1985), "Proposed West Beach Marina Hydraulic Model Investigation," James K. K. Look Laboratory of Oceanographic Engineering Technical Report No. 59, University of Hawaii.

Mei, C. C. (1983), "The Applied Dynamics of Ocean Surface Waves," John Wiley & Sons.

Shaw, R. P. (1976), "Long Period Forced Harbor Oscillations," Topics in Ocean Engineering (ed. Bretschneider, C. L.), Gulf Publishing Co., Texas, Vol. 3, pp. 29-40.

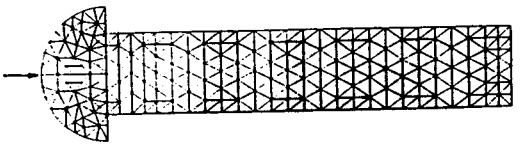

Figure 1 Discretization of the Rectangular Harbor with Triangular Elements

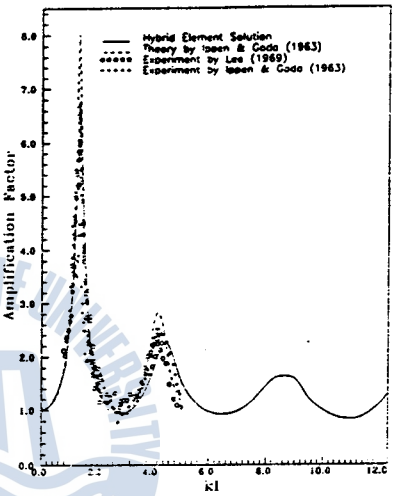

Figure 2 Response Curve for a Fully Open Rectangular Harbor with the Values of $K_r = 1.0, \beta = 0.0$

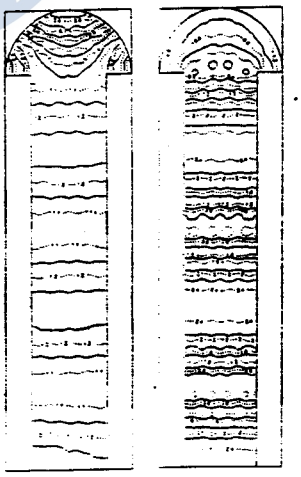

Figure 3 Contours of Wave Height Amplification Factor for a 0.4 sec Wave (a: Closed End, b: Open End)

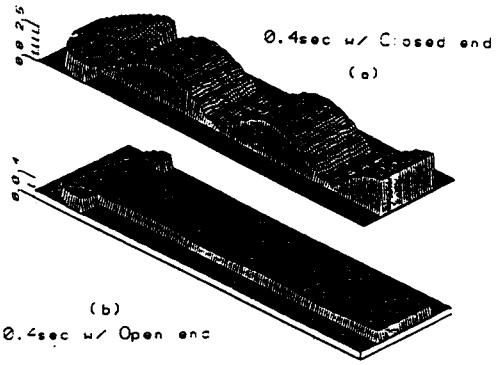

Figure 4 Surface Patterns of a 0.4 sec Wave (a: Closed End, b: Open End)

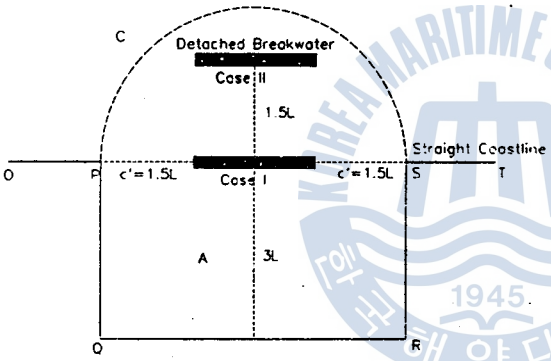

Figure 5 Arrangement of A Detached Breakwater for the Model (Cases I & II)

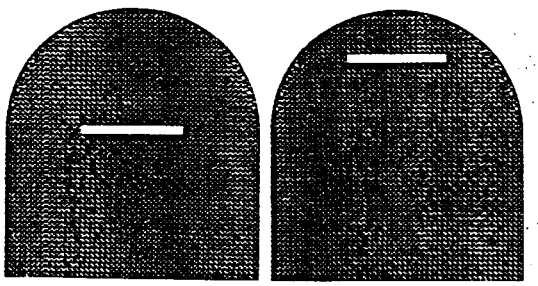

(a) Case I (b) Case II

Figure 6 Discretization of Rectangular Basin with A Detached Breakwater (Cases I & II)

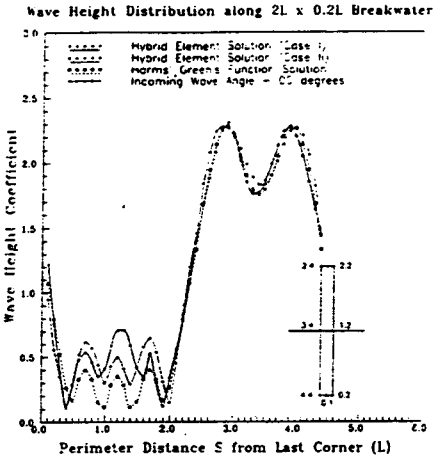

Figure 7 Comparison of the Numerical Solutions for Incident Waves Normal to the Detached Breakwater

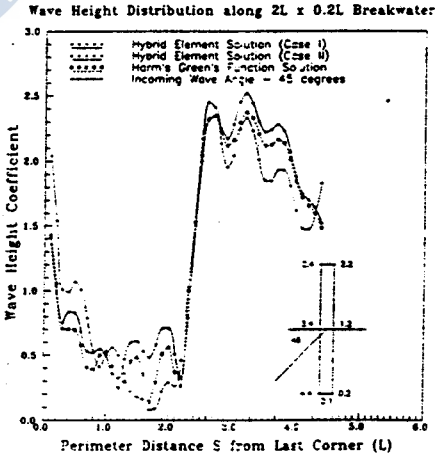

Figure 8 Comparison of the Numerical Solutions for Incident Waves directed $\theta = 45°$

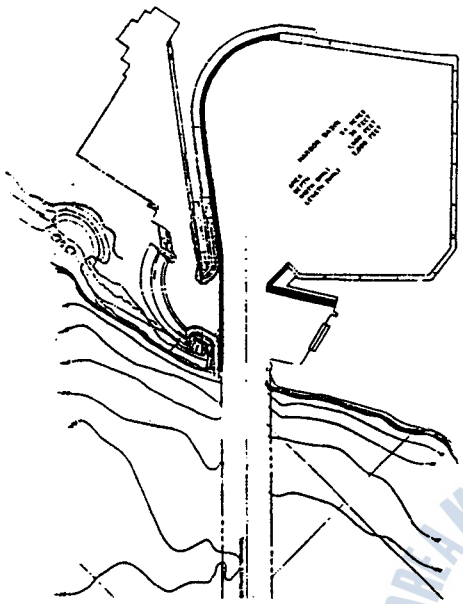

Figure 9 Model Application Area - Barbers Point Deep Draft Harbor and Barge Harbor, Oahu, Hawaii

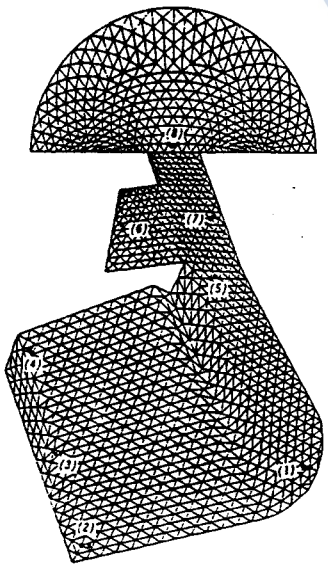

Figure 10 Location and Station Number for Wave Amplification (●) and Horizontal Velocities (*) at Barbers Point Harbor

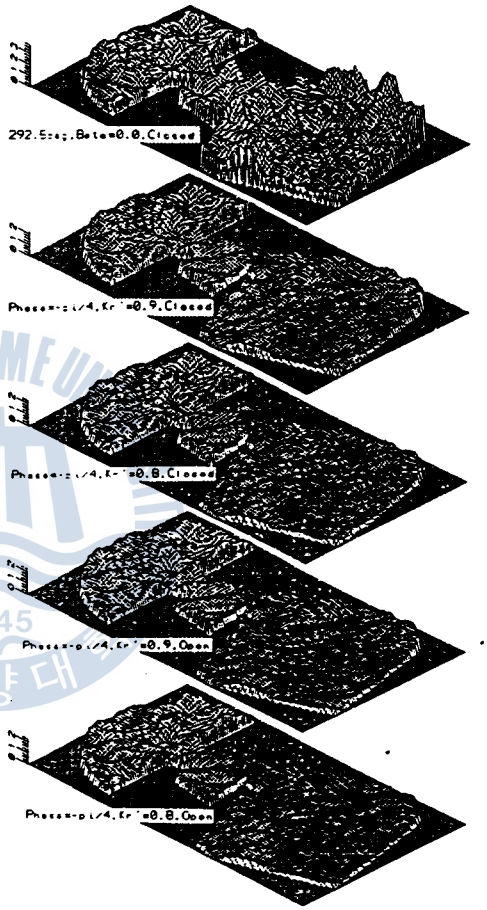

Figure 11 Surface Patterns for Barbers Point Harbor for $K_r = 0.98$, $\beta = 0.1$, $\gamma = -\frac{\pi}{4}$ and Various Values of K_r', and Entrance to West Beach Marina

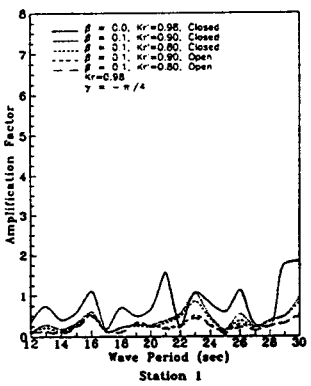

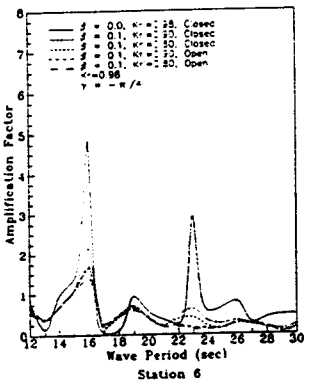

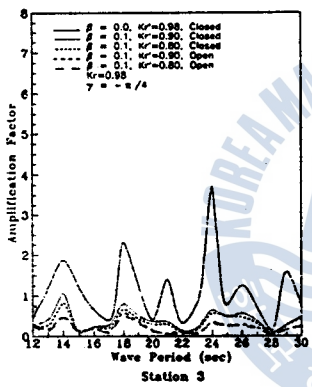

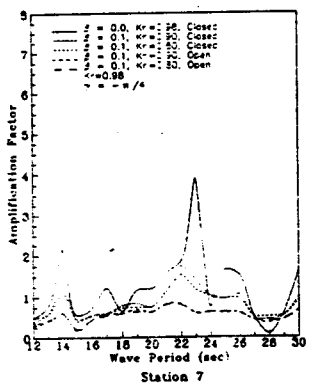

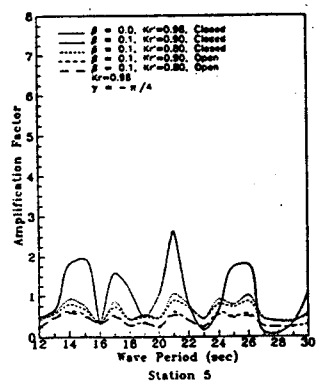

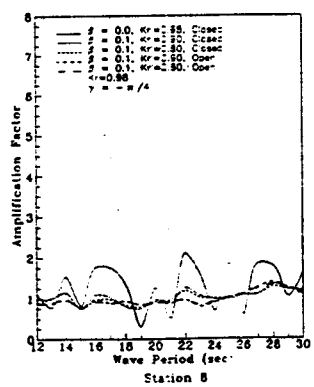

Figure 12 Frequency Response Curves - Wave Height Amplification Factor for Barbers Point Harbor for $K_r = 0.98$, $\beta = 0.1$, $\gamma = -\frac{\pi}{4}$, and Various Values of K_r', and Open Entrance to West Beach Marina

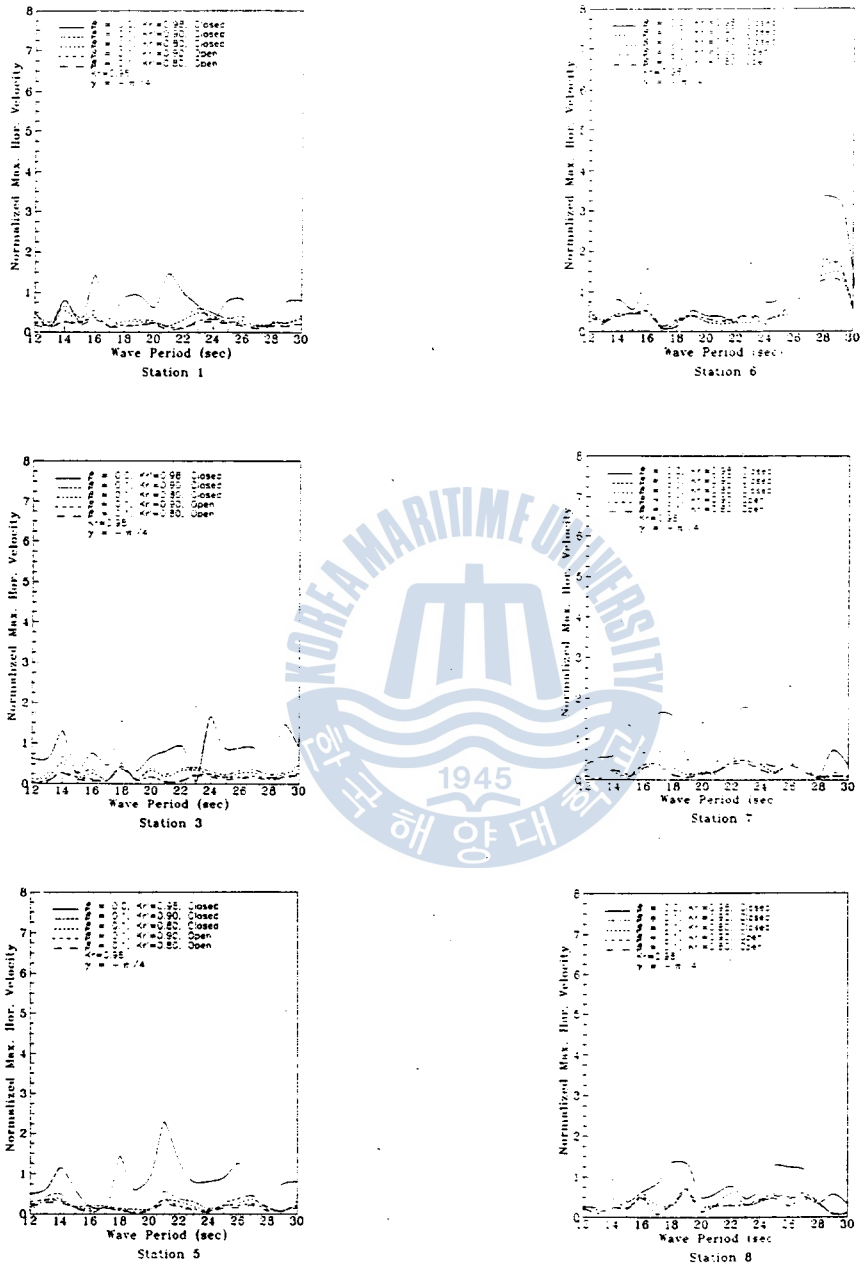

Figure 13 Frequency Response Curves - Normalized Maximum Horizontal Velocity for Barbers Point Harbor for $K_r = 0.98$, $\beta = 0.1$, $\gamma = -\frac{\pi}{4}$, and Various Values of K_t, and Open Entrance to West Beach Marina